Parametric gain control of a pulse in birefringent photonic crystal fibers

S. Coulibaly,[1] Z. Liu,[1] M. Taki,[1] and G. P. Agrawal[2]

[1]*Laboratoire de Physique des Lasers, Atomes et Molécules, CNRS UMR 8523, Université de Lille 1 Sciences et Technologies, 59655 Villeneuve d'Ascq Cedex, France*

[2]*The Institute of Optics, University of Rochester, Rochester, New York 14627, USA*

(Received 11 May 2012; published 4 September 2012)

Propagation of a modulationally amplified Gaussian pulse is considered inside a birefringent optical fiber. We show analytically that, in addition to a reduction in the parametric gain and a change in the pulse's group velocity, the third-order dispersion allows the generation of a temporal Airy-shaped pulse. Furthermore, pulse spreading in the temporal domain and chirping in the spectral domain both can be controlled through an interplay between third-order dispersion and modulational instability.

DOI: 10.1103/PhysRevA.86.033802 PACS number(s): 42.65.Sf, 42.55.Tv, 42.55.Wd, 42.81.−i

I. INTRODUCTION

The process by which a homogeneous state breaks up into a periodic state is known as modulational instability (MI) [1,2]. During its 40-year history, MI has been reported in both the space and time domains using numerous physical systems, including hydrodynamics, plasma physics, nonlinear optics, and Bose-Einstein condensation, just to cite a few. From a technological point of view, MI plays an important role in telecommunication systems. Indeed, in the experimental evidence for its occurrence in optical fibers, MI was shown to initiate pulse-train generation [3]. Since then, other potential applications of MI have been reported in the context of fiber-optic parametric amplifiers [4,5], supercontinuum (SC) generation [6], and optical rogue-wave formation [7].

In the context of fiber optics, MI is physically understood as a balance between the nonlinear and linear dispersive effects experienced by an optical field during its propagation. Mathematically, the propagation of light in a single-mode fiber is commonly modeled by the nonlinear Schrödinger (NLS) equation, and MI can only rise in the anomalous group-velocity-dispersion (GVD) regime. However, in the normal-dispersion regime the phase-matching condition underlying MI can be realized by adding an additional degree of freedom to the system. For example, Coen and Haelterman [8] predicted and experimentally observed that MI can be produced in a normally dispersive optical fiber by applying specific boundary conditions. An intrinsic characteristic of the optical fiber can also be used to obtain a supplementary degree of freedom. Indeed, the usual scalar NLS model results from a simplification that assumes that the polarization state of light does not change during its propagation. It is well known that real fibers exhibit modal birefringence with random changes in its magnitude and orientation along the fiber length.

In specifically designed photonic crystal fibers (PCF), the built-in birefringence can be made much larger than random birefringence variations, and one must consider the vectorial nature of wave propagation in such strongly birefringent fibers. In this case, the copropagating orthogonally polarized fields are found to exhibit the MI in cases of both normal and anomalous GVD [9–12]. From a theoretical point of view the case of orthogonally polarized fields has the advantage that it can be easily compared to the case of two continuous-wave (cw) pumps interacting inside an ideal optical fiber through cross-phase modulation [12].

In cases of both normal and anomalous GVD, MI gain was commonly thought to be unaffected by odd-order dispersion experienced by light during its propagation in a nonlinear Kerr medium. In fact, the MI gain is generally obtained through a standard linear stability analysis applicable only when the process is initiated by a monochromatic extended perturbation (cw pumping). Very recently, it has been shown that a proper accounting of the linear distortion effects and interactions experienced by different spectral components of a pulse yields a dramatic reduction of the MI gain in the presence of the third-order dispersion (slope of the GVD curve) [13].

In this paper we are interested in the third-order dispersion (TOD) effects on the pulse-seeded modulational instability process in a weakly birefringent fiber. We show that, in addition to a reduction of the MI gain previously predicted, distortion of the pulse shape under the TOD effects is described by an Airy function. More importantly, we show here that the pulse characteristics (width, chirp, etc.) can be controlled by an interplay between TOD and MI. This paper is organized as follows. In Sec. II, we recall the vectorial equations governing the propagation of orthogonal components of an arbitrary polarized light in a single-mode birefringent fiber. The background of linear stability analysis and general solutions of the linearized equation, given an initial perturbation, are presented. Section III is devoted to explicit calculations of the shape of a modulationally amplified Gaussian pulse, and the results are compared with numerical investigations of the vectorial equations in Sec. IV. Finally, the main results are summarized in Sec. IV.

II. POLARIZATION INSTABILITY

We start with the coupled generalized NLS equations satisfied by the orthogonally polarized components of a pulse in a lossless, birefringent optical fiber [9–12]:

$$\frac{\partial U}{\partial z}+\beta_{1x}\frac{\partial U}{\partial \tau}=i\beta\left(i\frac{\partial}{\partial\tau}\right)U+i\gamma\left(|U|^2+\frac{2}{3}|V|^2\right)U+i\frac{\gamma}{3}U^*V^2e^{-2i\Delta\beta z}, \tag{1a}$$

$$\frac{\partial V}{\partial z}+\beta_{1y}\frac{\partial V}{\partial \tau}=i\beta\left(i\frac{\partial}{\partial\tau}\right)V+i\gamma\left(|V|^2+\frac{2}{3}|U|^2\right)V+i\frac{\gamma}{3}U^2V^*e^{2i\Delta\beta z}. \tag{1b}$$

Here $U(z,\tau)$ and $V(z,\tau)$ stand for the two orthogonal components of an arbitrary polarized optical field $\mathbf{E}(z,t)$ at the carrier frequency ω_0, i.e.,

$$\mathbf{E}(z,t) = \tfrac{1}{2}\left[U(z,\tau)\,\hat{x} + V(z,\tau)\,\hat{y}\right] e^{i(\beta_0 z - \omega_0 t)} + \text{c.c.},$$

where $\beta_0 = (\beta_{0x} + \beta_{0y})/2$ is the average propagation constant, $\Delta\beta = (\beta_{0x} - \beta_{0y})/2 = 2\pi/L_B$ is a measure of the modal birefringence, and L_B is the birefringence length. The nonlinear parameter γ is proportional to the nonlinear refractive index responsible for the Kerr effect, and the dispersion operator $\beta(i\frac{\partial}{\partial\tau})$ is given by

$$\beta\left(i\frac{\partial}{\partial\tau}\right) = \sum_{n\geqslant 2}\frac{\beta_n}{n!}\left(i\frac{\partial}{\partial\tau}\right)^n.$$

Since we consider in this paper optical fibers with a relatively low birefringence, the group velocities β_{1x} and β_{1y} are nearly identical, and we set ($\beta_{1x} \approx \beta_{1y} = \beta_1$). Introducing $\bar{U} = U\exp(i\,\Delta\beta z/2)$ and $\bar{V} = V\exp(-i\,\Delta\beta z/2)$, the coupled equations describing the left and right circular polarizations $A_\pm = \left(\bar{U} \pm i\,\bar{V}\right)/\sqrt{2}$ are analogous to that of cross-phase modulation [12].

Equations (1) have a homogeneous cw solution corresponding to a constant-power mode whose polarization state is oriented along one of the principal axes. In what follows, we choose this polarization state along the y axis, which represents the fast (slow) axis for $\Delta\beta > 0$ ($\Delta\beta < 0$). Then the cw solution is given by $(U_0, V_0) = [0, \sqrt{P_0}\exp(i\gamma P_0 Z)]$, where P_0 is the mode power. To examine the stability of this state, let us introduce the perturbations to U_0 and V_0 in the following form:

$$U(Z,\tau) = u(Z,\tau), \tag{2a}$$
$$V(Z,\tau) = [\sqrt{P_0} + v(Z,\tau)]e^{i\gamma P_0 Z}, \tag{2b}$$

with $u(Z,\tau)$ and $v(Z,\tau)$ taken to be small in comparison to P_0 and $Z = z - \tau/\beta_1$. Inserting Eqs. (2) in Eqs. (1) and linearizing in u and v, we obtain the following uncoupled equations:

$$\frac{\partial\bar{u}}{\partial Z} = i\beta\left(i\frac{\partial}{\partial\tau}\right)\bar{u} + i\left(\Delta\beta - \frac{\gamma_0}{3}\right)\bar{u} + i\frac{\gamma_0}{3}\bar{u}^*, \tag{3a}$$
$$\frac{\partial v}{\partial Z} = i\beta\left(i\frac{\partial}{\partial\tau}\right)v + i\gamma_0(v + v^*), \tag{3b}$$

where we have set $\bar{u} = u\exp[i\,(\Delta\beta - \gamma_0)\,Z]$ and $\gamma_0 = \gamma P_0$. Equation (3b) is typically obtained when the scalar NLS equation is considered. Since we are concerned here with the normal-dispersion region, this equation excludes polarization instability of perturbations of the fast-axis component. Hence, the polarization instability in this case can be completely described by its component along the x axis.

In the frequency domain, Eq. (3a) together with its complex conjugate can be written in the form

$$\partial_Z\begin{bmatrix}\tilde{\bar{u}}(Z,\Omega)\\ \tilde{\bar{u}}^*(Z,-\Omega)\end{bmatrix} = \begin{bmatrix}M(\Omega) & i\gamma_0/3\\ -i\gamma_0/3 & M^*(-\Omega)\end{bmatrix}\begin{bmatrix}\tilde{\bar{u}}(Z,\Omega)\\ \tilde{\bar{u}}^*(Z,-\Omega)\end{bmatrix},$$

where $M(\Omega) = i\left[\beta(\Omega) + \Delta\beta - \gamma_0/3\right]$ and $\beta(\Omega)$ is the Fourier transform of the dispersion operator. Looking for solutions of the form

$$\begin{bmatrix}\tilde{\bar{u}}(Z,\Omega)\\ \tilde{\bar{u}}^*(Z,-\Omega)\end{bmatrix} = e^{\lambda Z}\begin{bmatrix}b_1\\ b_2\end{bmatrix},$$

we find that the eigenvalues λ can be written in the form

$$\lambda_\pm = -i\beta_a(\Omega) \pm g(\Omega), \tag{4}$$

where $g(\Omega) = [\beta_s(\Omega) + \Delta\beta]\,[2\gamma_0/3 - \Delta\beta - \beta_s(\Omega)]$ and we have defined the symmetric and asymmetric parts of $\beta(\Omega)$ as $\beta_a = [\beta(\Omega) - \beta(-\Omega)]/2$ and $\beta_s = [\beta(\Omega) + \beta(-\Omega)]/2$. Since we are interested in the amplification (or damping) of perturbations, we should consider only the eigenvalues with a nonzero real part, which correspond to $g(\Omega) \geqslant 0$. The corresponding solutions can be written as

$$\tilde{\bar{u}}(Z,\Omega) = F(Z,\Omega)\,\tilde{\bar{u}}(0,\Omega) + G(Z,\Omega)\,\tilde{\bar{u}}^*(0,-\Omega), \tag{5}$$

with

$$F(Z,\Omega) = e^{i\beta_a Z}\left(\cosh[g(\Omega)Z] + i\frac{\beta_s + \Delta\beta - \gamma_0/3}{g(\Omega)}\sinh[g(\Omega)Z]\right), \tag{6a}$$
$$G(Z,\Omega) = i\,e^{i\beta_a Z}\frac{\gamma_0/3}{g(\Omega)}\sinh[g(\Omega)Z]. \tag{6b}$$

Keeping the dispersion terms up to third order, $\beta(\Omega)$ can be written as $\beta(\Omega) = \beta_2\Omega^2/2 + \beta_3\Omega^3/6$. Then we have $\beta_a(\Omega) = \beta_3\Omega^3/6$ and $\beta_s(\Omega) = \beta_2\Omega^2/2$. Next, defining a dimensionless parameter $p = P_0/P_c$ with $P_c = 3\,|\Delta\beta|/2\gamma$, the parametric gain $g(\Omega)$ takes the explicit form

$$g(\Omega) = |\Delta\beta|\sqrt{\left(\mu\frac{\Omega^2}{\Omega_{c1}^2} + 1\right)\left(\mu p - 1 - \mu\frac{\Omega^2}{\Omega_{c1}^2}\right)}, \tag{7}$$

where $\mu = \text{sgn}(\Delta\beta) = \pm 1$ and $\Omega_{c1} = \sqrt{2|\Delta\beta|/\beta_2}$. For $\mu = 1$ corresponding to the polarization state along the fast axis, the instability band is given by $-\Omega_{c1}\sqrt{p-1} \leqslant \Omega \leqslant \Omega_{c1}\sqrt{p-1}$, and the maximum gain is obtained at $\Omega_c = \Omega_{c1}\sqrt{(p-2)/2}$. Modulation instability with $\Omega_c \neq 0$ is possible only when $p \geqslant 2$; otherwise, for $p \leqslant 2$, $\Omega_c = 0$. When the polarization is along the slow axis $\mu = -1$, one may observe two sidebands such that $-\Omega_{c1} \leqslant \Omega \leqslant \Omega_{c1}\sqrt{p+1}$ and $-\Omega_{c1}\sqrt{p+1} \leqslant \Omega \leqslant \Omega_{c1}$, and the gain is maximum at $\Omega_c = \pm\Omega_{c1}\sqrt{(p+2)/2}$. In this case, modulation instability occurs whenever $p \geqslant 0$. In the following we show how the TOD affects drastically the dynamics as soon as perturbations are localized (in the form of pulses).

III. TIME-DEPENDENT PERTURBATIONS

According to Eq. (5), we can compute the output solution given any known form of the initial perturbation. To stress on the effects of the TOD, we consider a simple case for which analytical calculations can be performed. More specifically, we set the initial perturbation in the form of a Gaussian shape,

$$\bar{u}(Z=0,\tau) = \bar{u}_0\exp\left[-\left(\frac{\tau}{2\tau_0}\right)^2 + i\Omega_0\tau\right], \tag{8}$$

whose Fourier transform is given by

$$\tilde{\bar{u}}\,(Z=0,\Omega)=2\sqrt{\pi}\,\tau_0\bar{u}_0\,\exp\left[-\tau_0^2\,(\Omega-\Omega_0)^2\right]. \quad (9)$$

Assuming the spectral bandwidth of the Fourier transform to be smaller than the MI bandwidth and the central frequency Ω_0 to be close to the most amplified frequency, we write $\Omega_0=\Omega_c+\delta\omega$, with $|\delta\omega|\ll|\Omega_c|$. Consequently, the parametric gain can be represented by its Taylor expansion

$$g_a\,(\Omega)=g_c+\frac{g''}{2}\,(\Omega-\Omega_c)^2+O\{(\Omega-\Omega_c)^3\}, \quad (10)$$

with $g_c=g\,(\Omega_c)$ and $g''=\partial^2 g\,(\Omega)/\partial\Omega^2\big|_{\Omega_c}$. The eigenvectors U and V take the form

$$F\,(Z,\Omega)\simeq F_c=\exp\left[i\frac{\beta_3}{6}\Omega^3 Z\right]\cosh[g_a\,(\Omega)\,Z], \quad (11a)$$

$$G\,(Z,\Omega)\simeq G_c=i\exp\left[i\frac{\beta_3}{6}\Omega^3 Z\right]\sinh[g_a\,(\Omega)\,Z]. \quad (11b)$$

Considering only the growing parts of the eigenvectors, we obtain the following explicit solution for the amplified perturbation [14,15]:

$$\bar{u}\,(Z,\tau)=\frac{2\bar{u}_0}{\sqrt{\pi}}\exp\left[i\frac{\beta_3}{6}\Omega_c^3 Z+\frac{p}{2}|\Delta\beta|Z-(\delta\omega\tau_0)^2\right]\left\{e^{i\Omega_c\tau}\int_{-\infty}^{\infty}\exp\left[iA\omega_-^2-\frac{i}{3}B\omega_-^3-(1+iC)\,\omega_-^2\right]d\omega_-\right.$$
$$\left.+ie^{-i\Omega_c\tau}\int_{-\infty}^{\infty}\exp\left[iA^*\omega_+-\frac{i}{3}B\omega_+^3-(1-iC^*)\omega_+^2\right]d\omega_+\right\}, \quad (12)$$

where we have set $\omega_\pm=(\Omega\pm\Omega_c)\,\tau_0$ and

$$A=\frac{\tau}{\tau_0}-\frac{\beta_3\Omega_c^2 Z+4i\delta\omega\tau_0^2}{2\tau_0}, \quad (13a)$$

$$B=\frac{\beta_3}{2\tau_0^3}Z=\frac{Z}{L_{\rm TOD}}, \quad (13b)$$

$$C=\frac{\beta_3\Omega_c+ig''}{2\tau_0^2}Z=\frac{\Omega_c\tau_0}{L_{\rm TOD}}Z-i\frac{(\beta_2\Omega_c)^2}{p\Delta\beta\tau_0^2}Z. \quad (13c)$$

Performing the integrals, we finally obtain

$$\bar{u}\,(Z,\tau)=\frac{\bar{u}_0\sqrt{\pi}}{|B|^{-1/3}}e^{p|\Delta\beta|Z/2-(\delta\omega\tau_0)^2}[\bar{u}_+e^{i\Omega_c\tau}+i\bar{u}_-e^{-i\Omega_c\tau}], \quad (14)$$

where

$$\bar{u}_+=e^{i\psi}\,\mathrm{Ai}[(1-AB-C^2+2iC)B^{-4/3}], \quad (15a)$$

$$\bar{u}_-=e^{-i\psi^*}\,\mathrm{Ai}[(1-A^*B-C^{*2}-2iC^*)B^{-4/3}], \quad (15b)$$

$$\psi=i\frac{\beta_3}{6}\Omega_c^3 Z+\frac{2-3AB-6C^2}{3B^2}-iC\frac{3AB+2C^2-6}{3B^2}, \quad (15c)$$

and $\mathrm{Ai}\,(x)$ is the Airy function. In contrast to the solution obtained in the context of pulse spreading [14], here all functions of the propagation length appearing in Eq. (14) are proportional to the TOD, suggesting that almost all characteristics may be affected by the latter. In addition, interplay between MI and pulse size allows further degrees of freedom for tuning the effects of the TOD. Of course in the expression (12), the drastic impact of TOD on the characteristics (e.g., amplitude, size, group velocity) of the output are included but hidden. However, for small or large values of B [see (13b)] asymptotic expressions can be found [14]. This approach is developed in the following and the predictions are compared with numerical simulations.

IV. NUMERICAL RESULTS

For numerical investigations we consider a birefringent fiber with a beat length of 2 m and γ value of 0.05 W^{-1} m^{-1}. Figure 1 shows solution (14) for increasing values of β_3 after one beat length. We also plot on the same graphs the results of numerical integration of Eqs. (1).

As can be expected and seen in Fig. 1, the numerical solutions are in very good agreement with analytical predictions. Note that in this range of parameters our solution is different from the one predicted in [13]. Indeed, the main expected result is a drastic reduction of the gain in the presence of the TOD. This reduction of the gain is accompanied by a change in the group velocity and a spreading of the pulse in time. The

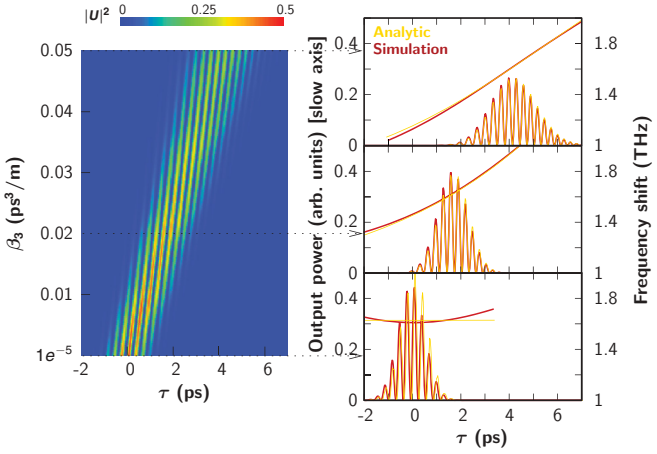

FIG. 1. (Color online) (left) Slow-axis power $|u(\tau)|^2$ as a function of β_3. (right) The pulse profiles (left axis) and instantaneous frequency shift (right axis) for $\beta_3=0.05$, 0.02, and 10^{-5} (from top to bottom). The parameters are $\beta_2=0.06$ ps^2/m, $\tau_0=0.5$ ps, $P_0=4P_c$, and perturbation is initialized to $u_0=1nW$. Red (dark gray) and yellow (light gray) lines are produced from numerical integration of Eqs. (1) and analytical predictions from (14), respectively.

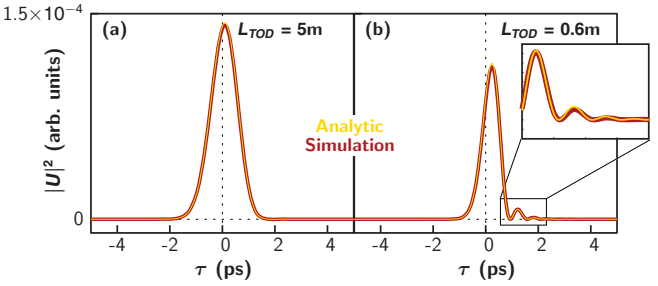

FIG. 2. (Color online) Numerical [yellow (light gray) lines] and analytical [red (dark gray) lines] pulse shapes along the slow axis after 2 m for (a) $\tau_0 = 0.5$ ps and (b) 0.25 ps. The other parameters are the same as in Fig. 1.

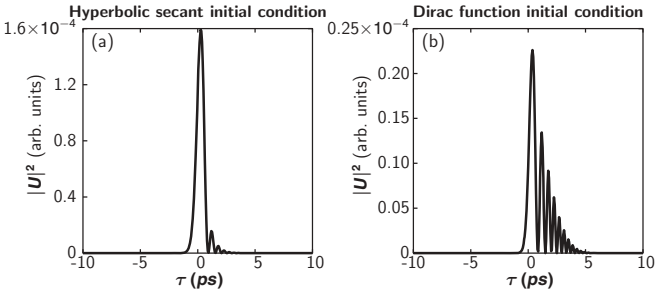

FIG. 4. Output intensity $|U|$ on the slow axis after 1.6 m for $p = 2.1$, corresponding to (a) a hyperbolic secant and (b) Dirac function initial conditions. The other parameters are the same as in Fig. 1.

origin of these effects can be understood by considering the dependence of A, B, and C on the TOD parameter. For the sake of simplicity, let us consider $\delta\omega = 0$. Then, A is nothing but the time variable normalized by the initial pulse width. Notice that time origin is now given by $\tau_{\max} = (\beta_3\Omega_c^2/2)Z$. This shift is the result of a TOD-induced change in the group velocity of the pulse.

The impact of TOD on the pulse profile results from a competition between the terms coming from B and C. Let us focus first on the case $C = 0$. This condition can be achieved when $\beta_2 = 0$ or $\Omega_c = 0$. However, since the presence of β_2 is necessary for the MI gain process, we will consider only the case $\Omega_c = 0$, which corresponds to $1 \leqslant p \leqslant 2$ when $\Delta\beta > 0$. B measures the propagation distance in units of the TOD length defined as $L_{\rm TOD} = 2\tau_0^3/\beta_3$. Figure 2(a) shows the analytical and numerical profiles for $Z/L_{\rm TOD} < 1$. As can be seen from Fig. 2(a) the pulse profile remains Gaussian. However, when $Z/L_{\rm TOD} > 1$ Airy oscillations become relevant, and the pulse displays an asymmetric profile seen in Fig. 2(b). In the spectral domain, a temporal Airy profile is known to introduce a frequency chirp. A typical evolution of the instantaneous frequency of the output beam is shown in Fig. 1 (see left axis of left panel). We can observe that the nonlinear chirp on the signal frequency is very well described by our analytical predictions.

Let us now investigate the effects of C when the propagation distances are much smaller than $L_{\rm TOD}$. When $\Delta\beta > 0$, the real

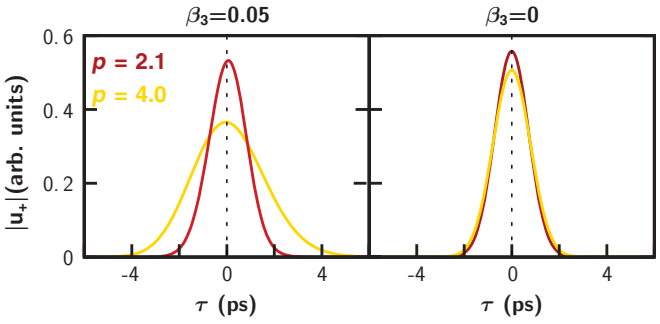

FIG. 3. (Color online) Amplitudes $|\bar{u}_\pm|$ on the slow axis after 1.6 m for $p = 2.1$ [yellow (light gray) lines], corresponding to $\Omega_c = 2.3$ THz, and $p = 4$ [red (dark gray) lines], corresponding to $\Omega_c = 10.2$ THz, (left) with and (right) without the TOD term. The other parameters are the same as in Fig. 1.

and imaginary parts of C can be consider independently since the TOD appears in the real part [see Eq. (13c)]. Keeping $Z/L_{\rm TOD} < 1$ and the mismatch parameter $\delta\omega = 0$, the impact of C can be singled out by varying Ω_c by means of p and considering the propagation with or without the TOD term. In Fig. 3 we show the impact of the real and imaginary parts of C on $\bar{u}_\pm$ by increasing the input power and, consequently, Ω_c. As can be seen from Fig. 3, in the absence of the TOD term [right graph; $\mathrm{Re}(C) = 0$], there is no significant change on the profile of the envelope when the imaginary part of C increases. In contrast, in the presence of the TOD [left graph; $\mathrm{Re}(C) \neq 0$] we observe that the envelope spreads out, suggesting that the major contribution of C to the pulse spreading comes from the real part, representing an interplay between the TOD and the MI frequency.

Finally, we emphasize that the results obtained here are not specific to the Gaussian shape of the initial condition. Figure 4 illustrates the pulse dynamics generated from two different initial conditions, namely, a hyperbolic secant [Fig. 4(a)] and a Dirac δ function [Fig. 4(b)]. As can be seen from Fig. 4, in both cases Airy oscillations develop.

V. CONCLUSIONS

We have carried out a theoretical description of the MI inside a birefringent fiber in the presence of the TOD term and a pulse-shape localized perturbation. Although the general case is characterized by an Airy-shaped profile, our result is consistent with previous results for a small value of the ratio between the propagation length and the TOD length. We have shown that the interplay between the TOD term and MI is responsible for a spreading of the pulse. The latter is very sensitive to the size of the initial pulse-like perturbation. In addition, our analytical results show that the pulse spreading can also be controlled by the input pump profile. We have also shown that the frequency chirp coming from the temporal Airy profile is rather nonlinear, and our predictions provide a good description of the phenomenon. Finally, we can assert that a birefringent fiber is a good medium for investigations of coupling between the MI and higher-order dispersion terms as it offers more degrees of freedom than a standard fiber. Finally, since almost all laser beams emit Gaussian pulses, the method can be successfully applied to a wide class of nonlinear multicomponent systems subject to time-reversal symmetry breaking.

[1] T. B. Feir and J. E. Benjamin, J. Fluid Mech. **27**, 417 (1967).
[2] K. Tai, A. Hasegawa, and A. Tomita, Phys. Rev. Lett. **56**, 135 (1986).
[3] E. J. Greer, D. M. Patrick, P. G. Wigley, and J. R. Taylor, Electron. Lett. **25**, 1246 (1989).
[4] J. E. Stolen and R. H. Bjorkholm, IEEE J. Quantum Electron. **18**, 1062 (1982).
[5] M. E. Marhic, N. Kagi, T.-K. Chiang, and L. G. Kazovsky, Opt. Lett. **21**, 573 (1996).
[6] J. M. Dudley, G. Genty, and S. Coen, Rev. Mod. Phys. **78**, 1135 (2008).
[7] D. R. Solli, C. Ropers, P. Koonath, and B. Jalali, Nature (London) **450**, 1054 (2007).
[8] S. Coen and M. Haelterman, Phys. Rev. Lett. **79**, 4139 (1997).
[9] S. Wabnitz, Phys. Rev. A **38**, 2018 (1988).
[10] J. E. Rothenberg, Phys. Rev. A **42**, 682 (1990).
[11] G. Millot, E. Seve, S. Wabnitz, and M. Haelterman, J. Opt. Soc. Am. B **15**, 1266 (1998).
[12] G. P. Agrawal, *Nonlinear Fiber Optics*, 3rd ed. (Academic, Boston, 2008).
[13] A. Mussot, A. Kudlinski, E. Louvergneaux, M. Kolobov, and M. Taki, Opt. Lett. **35**, 1194 (2010).
[14] M. Miyagi and S. Nishida, Appl. Opt. **18**, 678 (1979).
[15] M. Abramowitz and I. A. Stegun, *Handbook of Mathematical Functions* (Dover, New York, 1970), pp. 446–475.